Article

Rapid Sample-Mixing Technique for Transient NMR and Photo-CIDNP Spectroscopy: Applications to Real-Time Protein Folding

K. Hun Mok, Toshio Nagashima, Iain J. Day, Jonathan A. Jones, Charles J. V. Jones, Christopher M. Dobson, and P. J. Hore

J. Am. Chem. Soc., **2003**, 125 (41), 12484-12492• DOI: 10.1021/ja036357v • Publication Date (Web): 20 September 2003

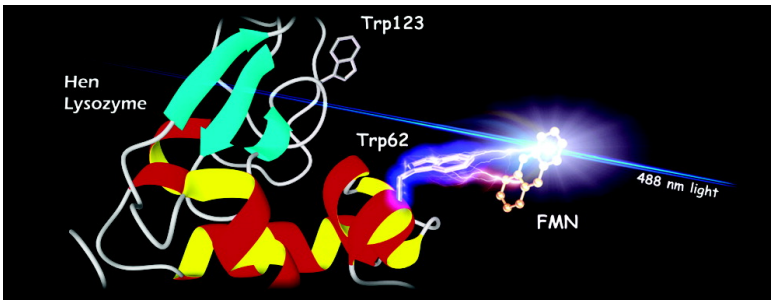

More About This Article

Additional resources and features associated with this article are available within the HTML version:

- Supporting Information
- Links to the 8 articles that cite this article, as of the time of this article download
- Access to high resolution figures
- Links to articles and content related to this article
- Copyright permission to reproduce figures and/or text from this article

View the Full Text HTML

J|A|C|S
ARTICLES
Published on Web 09/20/2003

Rapid Sample-Mixing Technique for Transient NMR and Photo-CIDNP Spectroscopy: Applications to Real-Time Protein Folding

K. Hun Mok,[†] Toshio Nagashima,[‡,⊥] Iain J. Day,[‡] Jonathan A. Jones,[†,§] Charles J. V. Jones,[‡] Christopher M. Dobson,[†,∥] and P. J. Hore*[,‡]

Contribution from the Oxford Centre for Molecular Sciences, University of Oxford, Central Chemistry Laboratory, South Parks Road, Oxford, OX1 3QH, United Kingdom, Oxford Centre for Molecular Sciences, University of Oxford, Physical and Theoretical Chemistry Laboratory, South Parks Road, Oxford, OX1 3QZ, United Kingdom, Centre for Quantum Computation, Department of Physics, University of Oxford, Clarendon Laboratory, Parks Road, Oxford OX1 3PU, United Kingdom, University Chemical Laboratory, University of Cambridge, Department of Chemistry, Lensfield Road, Cambridge, CB2 1EW, United Kingdom

Received May 27, 2003

Abstract: We describe the development and application of a novel rapid sample-mixing technique for real-time NMR (nuclear magnetic resonance) spectroscopy. The apparatus consists of an insert inside a conventional NMR tube coupled to a rapid injection syringe outside the NMR magnet. Efficient and homogeneous mixing of solutions in the NMR tube is achieved with a dead time of tens of milliseconds, without modification of the NMR probe or additional hardware inside the magnet. Provision is made for the inclusion of an optical fiber to allow in situ laser irradiation of samples, for example to generate photo-CIDNP (chemically induced dynamic nuclear polarization). An NMR water suppression method has been implemented to allow experiments in H_2O as well as in deuterated solvents. The performance of the device has been tested and optimized by a variety of methods, including sensitive detection of residual pH gradients and the use of NMR imaging to monitor the extent of mixing in real time. The potential utility of this device, in conjunction with the sensitivity and selectivity of photo-CIDNP, is demonstrated by experiments on the protein hen lysozyme. These measurements involve the direct detection of spectra during real-time refolding, and the use of CIDNP pulse labeling to study a partially unfolded state of the protein under equilibrium conditions. Magnetization transfer from this disordered state to the well-characterized native state provides evidence for the remarkable persistence of nativelike elements of structure under conditions in which the protein is partially denatured and aggregation prone.

Introduction

The mechanism by which proteins fold has attracted much experimental and theoretical attention in recent years[1,2] Significant insights into how a polypeptide chain attains its unique, compact three-dimensional structure have come from a variety of physical techniques including fluorescence, circular dichroism, and nuclear magnetic resonance (NMR) spectroscopy.[3,4,5] NMR has proven to be particularly powerful by virtue of the residue-specific, atomic-level structural and dynamical information afforded by chemical shifts, spin−spin couplings, and spin relaxation. Usually, NMR is applied to equilibrium states of proteins. Pulsed hydrogen/deuterium exchange, for example, has been used to great effect to probe the existence and dynamics of secondary structure in non-native states of proteins.[6] Powerful and general though such approaches are, NMR also has the potential to probe transient nonequilibrium intermediates formed during the folding process, provided folding can be initiated and spectra can be recorded sufficiently rapidly. Such real-time NMR techniques provide the opportunity to follow changes in the local environment and dynamics of individual atoms as the native backbone-fold is formed and as side chains become closely packed.[4,5,7]

Probably the most general and versatile form of real-time NMR as applied to proteins involves triggering folding by means

* peter.hore@chem.ox.ac.uk.
[†] Oxford Centre for Molecular Sciences, University of Oxford, Central Chemistry Laboratory.
[‡] Oxford Centre for Molecular Sciences, University of Oxford, Physical and Theoretical Chemistry Laboratory.
[§] Centre for Quantum Computation, Department of Physics, University of Oxford, Clarendon Laboratory.
[∥] University Chemical Laboratory, University of Cambridge, Department of Chemistry.
[⊥] Current address: Protein Research Group, RIKEN, 1−7−22 Suehirocho, Tsurumi-ku, Yokohama, 230-0045, Japan.

(1) Dobson, C. M.; Karplus, M. *Curr. Opin. Struct. Biol.* **1999**, *9*, 92−101.
(2) Dinner, A. R.; Salí, A.; Smith, L. J.; Dobson, C. M.; Karplus M. *Trends Biochem. Sci.* **2000**, *25*, 331−339.
(3) Brockwell, D. J.; Smith D. A.; Radford S. E. *Curr. Opin. Struct. Biol.* **2000**, *10*, 16−25.
(4) van Nuland, N. A. J.; Forge, V.; Balbach, J.; Dobson, C. M. *Acc. Chem. Res.*, **1998**, *31*, 773−780.
(5) Dobson C. M.; Hore, P. J. *Nat. Struct. Biol.* **1998**, *5*, 504−507.
(6) Englander, S. W. *Annu. Rev. Biophys. Biomol. Struct.* **2000**, *29*, 213−238.
(7) Frieden, C.; Hoeltzli S. D.; Ropson, I. J. *Protein Sci.* **1993**, *2*, 2007−2014.

10.1021/ja036357v CCC: $25.00

of an abrupt change in the concentration of one or more species in solution. Denatured proteins can be induced to refold in vitro by rapid dilution of a chemical denaturant, by the addition of metal ions or by a pH-jump.[7−11] For example, in a recent study of α-lactalbumin, a partially folded kinetic folding intermediate was detected following dilution from 6 M guanidinium chloride.[8] The native state evolved in a cooperative manner from the intermediate which was formed in the dead-time of the experiment; the kinetics of folding were closely similar to those observed by stopped-flow fluorescence and near UV circular dichroism. Related experiments, on a somewhat faster time scale, have been performed by exploiting the photo-CIDNP (Chemically Induced Dynamic Nuclear Polarization) effect[12] to probe, additionally, changes in the accessibility of aromatic side chains as folding progresses.[13,14]

The ability of perform nonequilibrium NMR measurements of this sort opens up many other possibilities for the study of proteins. Just as it is possible to transfer nuclear polarization or coherence within or between stable molecules engaged in conformational or chemical equilibria, so one can transfer magnetization from one state of a protein to another by means of a sudden perturbation. An example is the two-dimensional SCOTCH (Spin COherence Transfer in CHemical reactions) experiment in which laser irradiation within an appropriate NMR pulse sequence allows light and dark states of photoactive proteins to be correlated.[15,16] Similar techniques have been devised using temperature jumps.[17] An alternative strategy, used to probe the structures of partially unfolded proteins whose NMR spectra are poorly resolved, is to label certain groups or regions of the unfolded state using radio frequency irradiation or CIDNP and then rapidly to refold the protein in order to observe the polarization in the well-resolved spectrum of the native state.[14,18]

Nonequilibrium and real-time NMR experiments with the sensitivity and spectral and temporal resolution required to study the transformations between different states of proteins are technically demanding. There are essentially two strategies for concentration-jump experiments: one is to adapt the three-syringe, T-piece technology common in optical stopped flow spectroscopy[19] to allow mixing of solutions outside the NMR probe and rapid delivery of the mixture into the radio frequency coil region.[20,21,22,23] The other approach is to use the NMR sample tube itself as the mixing chamber. The simplest method involves injection of one solution into another in the NMR tube so that the ensuing turbulence causes homogeneous and rapid mixing.[8,24,25] Other, more sophisticated techniques use moving parts inside the NMR coil region to permit physically separate solutions to mix.[26,27] Whichever way the mixing is done, there are a number of challenges associated with minimizing the experimental dead time required for homogeneous mixing without unduly compromising the spectral resolution or detection sensitivity by probe modifications or the presence of reactant delivery tubing near the radio frequency coil. These difficulties are exacerbated by the "one-shot" nature of most of these real-time experiments, which offer little scope for signal averaging.

In this paper, we present a new design of rapid-mixing device for real-time NMR. The apparatus consists of an insert placed inside a conventional 5 mm NMR tube coupled to a rapid injection syringe positioned outside the NMR magnet. The insert design and construction allows efficient and homogeneous mixing of solutions in the NMR tube with a dead time of tens of milliseconds, without modification of the NMR probe or additional hardware inside the magnet. There is also provision for inclusion of an optical fiber to allow in situ light irradiation of samples, for example to generate CIDNP. A variety of benchmark measurements have been performed to test and optimize the performance of the device, including sensitive detection of residual pH gradients in an unbuffered sample with pH-sensitive chemical shifts and the use of one-dimensional ^{1}H NMR imaging to monitor the extent of mixing in real time. The performance of the technique is demonstrated by means of two experiments, on very different time scales, to study the structure of partially unfolded states of hen lysozyme. Although the discussion here focuses on proteins, one can imagine a variety of chemical applications in which reactions could be initiated by mixing of solutions and monitored by NMR on a 100 ms time scale with or without simultaneous light irradiation.

Materials and Methods

A. Materials. *N*-α-acetyl-L-histidine (N−Ac−His), flavin mononucleotide (FMN; sodium salt), and hen egg white lysozyme (HEWL; 3× crystallized) were purchased from Sigma and used without further purification. Tris(hydroxymethyl-d_3)-amino-d_2-methane (*d*-Tris; 1.0 M solution) was purchased from Isotec Inc. Guanidine HCl (Sequanal grade, 8.0 M pre-made solution) was purchased from Pierce Chemical Co. Deuterium oxide (D_2O) was obtained from Apollo Scientific Ltd. The chemical shift reference compounds 1,4-dioxane and 2,2-dimethyl-2-silapentane-5-sulfonate (DSS) were purchased from Aldrich. NMR sample tubes were obtained from Shigemi Inc. (BMS-005V, Allison Park, PA). All other chemicals were purchased from either Sigma or Aldrich and were of the highest grades available.

B. Digital Video Recording. Video footage was recorded using a Sony DCR-TRV310 digital video camera, with frame capturing at 30 Hz performed using iMovie (v. 2.1.1, Apple Computer Inc.) on a Macintosh PowerPC G3 desktop computer.

C. NMR Spectroscopy and Photo-CIDNP Experiments. The experiments described in this paper were performed on home-built NMR spectrometers at the Oxford Centre for Molecular Sciences, operating at ^{1}H frequencies of 500.1 and 600.1 MHz. The ^{1}H NMR probes were

(8) Balbach, J.; Forge, V.; van Nuland, N. A. J.; Winder, S. L.; Hore P. J.; Dobson, C. M. *Nature Struct. Biol.* **1995**, *2*, 865−870.
(9) Wirmer, J.; Kühn T.; Schwalbe H. *Angew. Chem., Int. Ed. Engl.* **2001**, *40*, 4248−4251.
(10) Balbach, J.; Forge, V.; Lau, W. S.; van Nuland, N. A. J.; Brew, K.; Dobson, C. M. *Science* **1996,** *274*, 1161−1163.
(11) Balbach, J. *J. Am. Chem. Soc.* **2000**, *122*, 5887−5888.
(12) Hore, P. J.; Broadhurst, R. W. *Prog. NMR Spectrosc.* **1993**, *25*, 345−402.
(13) Hore, P. J.; Winder, S. L.; Roberts, C. H.; Dobson, C. M.; *J. Am. Chem. Soc.*, **1997**, *119*, 5049−5050.
(14) Lyon, C. E.; Suh, E.-S.; Dobson, C. M.; Hore, P. J. *J. Am. Chem. Soc.* **2002**, *124*, 13 018−13 024.
(15) Kemmink, J.; Vuister, G. W.; Boelens, R.; Dijkstra, K.; Kaptein R.; *J. Am. Chem. Soc.* **1986**, *108*, 5631−5633.
(16) Rubenstenn, G.; Vuister, G. W.; Mulder, F. A. A.; Düx, P. E.; Boelens, R.; Hellingwerf, K. J.; Kaptein, R. *Nat. Struct. Biol.* **1998**, *5*, 568−570.
(17) Kawakami, M.; Akasaka, K. *Rev. Sci. Instrum.* **1998**, *69*, 3365−3369.
(18) Balbach, J.; Forge, V.; Lau, W. S.; Jones, J. A.; van Nuland, N. A. J.; Dobson, C. M. *Proc. Natl. Acad. Sci. U.S.A.* **1997**, *94*, 7182−7185.
(19) Chance, B. *J. Franklin Inst.* **1940**, *229*, 455−478, 613−640, 737−766.
(20) Grimaldi, J.; Baldo, J.; McMurray, C.; Sykes, B. D. *J. Am. Chem. Soc.* **1972**, *94*, 7641−7645.
(21) Kühne, R. O.; Schaffhauser, T.; Wokaun, A.; Ernst, R. R. *J. Magn. Reson.* **1979**, *35*, 39−67.
(22) McGee, W. A.; Parkhurst, L. J. *Anal. Biochem.* **1990**, *189*, 267−273.
(23) Hoeltzli, S. D.; Ropson, I. J.; Frieden, C. In *Techniques in Protein Chemistry* V.; Crabb, J. W., Ed.; Academic Press: New York, 1994; pp 455−465.
(24) Couch, D. A.; Howarth, O. W.; Moore P. *J. Phys. E* **1975**, *8*, 831−833.
(25) McGarrity, J. F.; Prodolliet, J.; Smyth,T. *Org. Magn. Reson.* **1981**, *17*, 59−65.
(26) Spraul, M.; Hofmann, M.; Schwalbe, H. U.S. Patent 5,726,570, 1998.
(27) Hamang, M.; Sanson, A.; Liagre, L.; Forge V.; Berthault, P. *Rev. Sci. Instrum.* **2000**, *71−5*, 2180−2183.

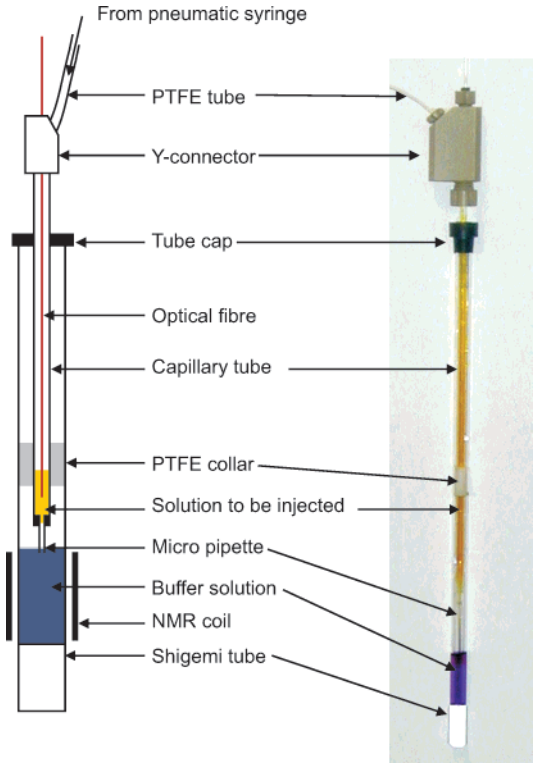

Figure 1. Schematic drawing and photograph of the coaxial injection insert inside a 5 mm diameter Shigemi tube.

equipped with a pair of double tuned Helmholtz coils for triple resonance inverse detection and were also fitted with triple axis field gradients (65 G cm^{-1}). The sample temperature was controlled by means of a homemade Peltier thermoelectric semiconductor device,[28] which maintained sample temperature in the range of 278−323 ± 0.1 K. All experiments were performed at 298 K. For photo-CIDNP experiments, laser illumination was provided by an argon ion laser (Spectra-Physics Stabilite 2016−05; principal wavelengths at 488 and 514 nm) operating in multiline mode with a power output of 5 W. Coupling to the NMR probe was achieved via an optical fiber (diameter 1 mm) and a mechanical shutter controlled by the spectrometer. All spectra were processed and analyzed using a combination of Felix 2.3 (MSI) and NMRPipe.[29]

D. Description of the Injection Device. The injection device consists of two major components: a coaxial glass insert fitted inside the NMR sample tube and a pneumatic injector placed outside the magnet. There is the option to add an optical fiber for photo-CIDNP experiments. Shigemi tubes (5 mm outside diameter, magnetic susceptibility matched to D_2O) were routinely used for two reasons. First, a smaller sample volume is required, which is advantageous when using precious and/or isotopically labeled samples. Second, when the jet of injected solution strikes the flat bottom of the tube, greater turbulence is produced than with a round-bottomed tube, improving the efficiency with which the solutions mix.

1. NMR Tube Insert. The coaxial insert, shown schematically and as a photograph in Figure 1, consists of glass capillary tubing (Wilmad, i.d. 1.6 mm, o.d. 2.0 mm) with one end fused to a 25 mm length of a glass micropipet (Blaubrand intraMARK) of 0.17 mm i.d. The liquid to be injected is held inside the capillary. This configuration introduces a highly collimated jet of liquid into the NMR tube during the injection. A PTFE collar (length, 1 cm) situated approximately two-thirds of the distance along the insert holds it coaxially within the NMR tube. The insert is supported at the top of the NMR tube by a standard tube cap, with a 2.5 mm hole drilled in the center. The tip of the pipet is positioned 1.5 mm above the top of the coil, so as to cause minimal disturbance to the field homogeneity, and just below the surface of the buffer solution in the NMR tube. A small air bubble (volume ≈ 0.5 μL) is introduced into the end of the micropipet to reduce diffusion of injectant into the buffer solution prior to the injection. The presence of the bubble was found to have no detectable effect on either the mixing efficiency or the signal intensity.

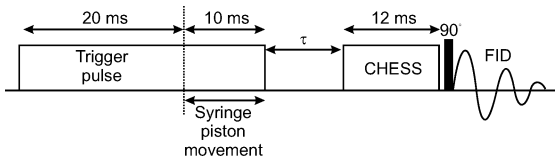

Figure 2. Timing diagram showing the voltage pulse used to trigger the injector and the motion of the syringe piston together with the proton RF pulses. The 20 ms delay is the time required for the pneumatic system to activate. The period τ is a delay to allow complete mixing within the NMR tube.

At the top of the glass capillary is a homemade HPLC-type Y-connector (polyethylene ether ketone, PEEK) into which is coupled a PTFE transfer line (internal diameter 0.5 mm) which feeds the injectant solution into the glass capillary. Optionally, an optical fiber can be inserted coaxially into the glass capillary for use in photo-CIDNP experiments. The bottom end of the optical fiber is held 27 mm above the micropipet piece using a rubber washer and locking nut on the top of the Y-connector. The optical fiber dips into the injectant solution, but only the cylindrical region immediately below the tip is irradiated with laser light. Introduction of light into the NMR sample can be used to induce the photochemical reactions that generate CIDNP enhancements for probing side chain accessibilities in proteins.[12,13] The PTFE transfer line is connected to a glass syringe in the pneumatic injector as described below.

2. Pneumatic Injector. The injector itself consists of a glass syringe (SGE 500R-GT) mounted in a block constructed from PTFE, stainless steel and PEEK. The PTFE tube from the insert is connected to the syringe by means of "heat-shrink" tubing, producing a watertight seal. The action of the syringe is governed by a pneumatic piston, controlled using a TTL line from the spectrometer, and driven by nitrogen gas at a pressure of 10 bar. Figure 2 shows a timing diagram for the injection. The minimum electronic gate time needed in the pulse sequence to depress the piston and to inject 50 μL of solution is 10 ms, with an inherent dead time of 20 ms due to the time required to activate the pneumatic system (see Results and Discussion below).

E. Solvent Suppression. Modern solvent suppression techniques that use "excitation sculpting" such as DPFGSE (Double Pulsed Field Gradient Spin−Echo),[30] or WATERGATE (WATER suppression through GrAdient Tailored Excitation)[31,32] are not readily compatible with rapid injection experiments. Both techniques rely on a gradient echo to dephase selectively the solvent magnetization, leaving the desired signals intact. Our experience has been that even 1 s after an injection, when the NMR spectrum shows that the two solutions are completely mixed, there is enough residual bulk motion of the liquid in the sample tube to prevent complete refocusing of the solute magnetization. These problems are similar to those encountered during in-vivo NMR spectroscopy, where they have been successfully circumvented using methods such as CHESS (CHEmical Shift Selective) excitation.[33] This procedure consists of a selective 90° pulse on the solvent resonance followed by a dephasing gradient, repeated three times using orthogonal gradients, prior to the acquisition pulse. In the

(28) Gregory, N. L.; Claridge, T. D. W.; Leonard, M. *J. Magn. Reson.* **1997**, *124*, 228−231.
(29) Delaglio, F.; Grzesiek, S.; Vuister, G. W.; Zhu, G.; Pfeifer, J.; Bax, A. *J. Biomol. NMR* **1995**, *6*, 277−293.
(30) Hwang, T.-L.; Shaka, A. J. *J. Magn. Reson. A.* **1994**, *112*, 275−279.
(31) Piotto, M.; Saudek, V.; Sklenar, V. *J. Biomol. NMR* **1992**, *2*−*6*, 661−665.
(32) Liu, M.; Mao, X.-a.; Ye, C.; Huang, H.; Nicholson, J. K.; Lindon, J. C. *J. Magn. Reson.* **1998**, *132*, 125−129.
(33) Haase, A.; Frahm, J.; Hänicke, W.; Matthaei, D. *Phys. Med. Biol.* **1985**, *30*, 341−344.

present case, CHESS solvent suppression allowed rapid injection NMR experiments to be performed very successfully in H_2O, so that solvent-exchangeable protons could be observed, e.g., the indole NH protons of tryptophan residues (as described below).

F. Procedures for the pH Jump Experiments. A 50-μL volume of 10 mM N−Ac−His, pH 4.0 (pH adjusted with 1.0 M DCl), containing 1,4-dioxane was injected into 280 μL of 0.15 M *d*-TrisDCl buffer, pH 8.5, containing DSS. Both solutions were prepared in D_2O. All pH measurements were uncorrected for the deuterium isotope effect. The final pH after injection was 8.3. Each ^{1}H NMR spectrum in the series was acquired separately using a fresh sample and a different postinjection delay. Such measurements, when displayed as a function of the delay time, are referred to as "pseudo real-time spectra", to differentiate them from "real-time spectra", where a single injection event is detected as a series of consecutively acquired signals (an example of the latter, in which the refolding of lysozyme is detected, is shown below). The number of complex data points was 256, and the spectral width was 5000 Hz, resulting in an acquisition time of 51.2 ms (see the Results section below for details). Forward−backward linear prediction and zero-filling were used to extend the data set to 4096 complex points. A cosine-squared window function was applied prior to Fourier transformation.

A similar experiment was subsequently carried out in the absence of Tris buffer. A 50-μL volume of 0.06% sodium deuterioxide solution containing DSS was injected into 280 μL of 10 mM N−Ac−His, pH 4.2 containing 1,4-dioxane. Both solutions were prepared in D_2O. The final pH of the solution after injection was 6.5. A series of pseudo real-time ^{1}H NMR spectra was acquired and processed as described above. A titration curve of chemical shift of the imidazole ring protons as a function of solution pH was obtained separately by systematically increasing the pH by addition of small aliquots of sodium deuterioxide to 10 mM N−Ac−His solution (pH 4.2).

G. One-Dimensional ^{1}H NMR Imaging. A 50-μL volume of H_2O was injected into 280 μL of D_2O. The spectra were recorded in real-time at 10 ms intervals using 256 complex points and a spectral width of 28 571.4 Hz. A weak field gradient ($\sim$2 G cm^{-1}) was applied along the appropriate axis (*x*, *y*, or *z*) during the acquisition of the free induction decays (FID).[34] A total of 256 FIDs were acquired for each experiment. Spectra were processed with a cosine-squared bell window function prior to Fourier transformation.

H. Real-Time Refolding of Hen Egg White Lysozyme. A 50-μL volume of 10 mM HEWL in 8.0 M guanidine HCl (pH 7.5), containing 0.2 mM FMN, 1,4-dioxane and 10% D_2O was injected into 280 μL of distilled H_2O containing 0.2 mM FMN and 10% D_2O. The final concentrations of HEWL and guanidine HCl were 1.5 mM and 1.5 M, respectively. The final pH of the solution containing the refolded protein was 6.5. A single injection of 20 ms duration was followed by a real-time series of photo-CIDNP spectra recorded every 340 ms (100 ms laser illumination given before each FID acquisition, with the end of the optical fiber placed 1 mm above the end of the capillary) for 23 s (64 spectra in total). A crush pulse was applied after the acquisition of each FID to remove the equilibrium magnetization, removing the need for the subtraction of a dark spectrum. The 600 MHz ^{1}H NMR spectra were acquired using 2048 complex points, a spectral width of 9009 Hz and averaged over four injections. The data set was extended to 4096 complex points using forward−backward linear prediction and exponential line broadening of 10 Hz was applied prior to Fourier transformation. Water suppression was provided by the CHESS sequence[33] as described above.

I. CIDNP Pulse Labeling of a Partially Folded State of Hen Egg White Lysozyme. A 50-μL volume of 6.4 mM HEWL in 45% 2,2,2-trifluoroethanol (TFE), pH 2, containing 0.15 mM FMN, 1,4-dioxane, and 10% D_2O was injected into 0.05 M sodium acetate buffer, pH 5.2, 10% D_2O. The final concentrations of HEWL and TFE were 1 mM and 7%, respectively. The final pH of the solution containing the refolded protein was 5.1. The spectrum was recorded at 600 MHz, as the difference between four light and four dark scans, all recorded separately. Laser illumination for 500 ms was used, with the injector activated for a time of 50 ms, which is sufficient for complete mixing to have occurred. A postinjection delay of 100 ms was used to allow refolding of the protein to the native state. The spectrum consisted of 4096 complex points and was processed with 5 Hz exponential line broadening prior to Fourier transformation.

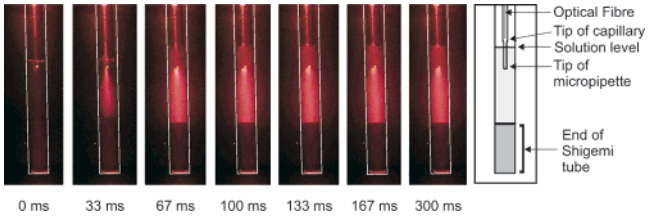

Figure 3. Frames captured from a digital video recording of an injection of methylene blue solution into water under laser illumination. (The images appear red as a result of the argon ion laser filter placed in front of the camera lens). The edge of the NMR tube is drawn as a white line to guide the eye. The injection event occurs between the first and second frames. Little change is observed beyond the third frame, indicating that the mixing is effectively complete within 67 ms.

Results and Discussion

A. Calibration of the Mixing Device. Several experiments were carried out to determine the efficiency with which the injection device mixes the injected liquid with the buffer solution in the NMR tube. A preliminary indication of the time scale of mixing was obtained by injecting a fluorescent dye solution while filming the event with a digital video camera. A separate series of experiments involved monitoring the time dependence of the ^{1}H NMR chemical shifts of histidine before, during and after a pH-jump, under conditions of fast exchange between the protonated and neutral forms of the imidazole ring. Finally, a real-time NMR imaging experiment was performed that provided spatial information on the distribution of the injected solution as it was being transferred into the NMR tube.

1. Digital Video Measurements. In the presence of low power laser illumination, methylene blue becomes fluorescent allowing the observation of high contrast images of the injection event. The concentration of methylene blue was chosen to give an optical density low enough that the laser illuminated the entire contents of the tube after the injection. A digital video recording of the injection event was made; consecutive frames (time interval 33.3 ms) are shown in Figure 3. In the 33 ms frame, the injection event is captured in the shape of a conical stream, which in the 67 ms frame is seen to reach the bottom of the Shigemi tube. Mixing is essentially complete within the time taken to record two frames (67 ms), there being no significant change in the video image in subsequent frames. The apparently uniform and homogeneous fluorescence suggests that the injected solution is efficiently transported to the bottom of the NMR tube and that mixing takes place throughout the sample volume. Similar experiments (results not shown) have also been performed by injecting aqueous samples of 8 M guanidine HCl and of 45% TFE, to reproduce the solvent conditions used in the real-time measurements on hen lysozyme reported below. In both cases, the mixing is a little slower, consistent with the higher viscosities of these solutions, but is complete within the time required to record three frames (100 ms).

(34) Mansfield, P.; Morris, P. G. NMR Imaging in Biomedicine; *Adv. Magn. Reson. Supp. 2*; Waugh, J. S., Ed.; Academic Press: New York, 1982.

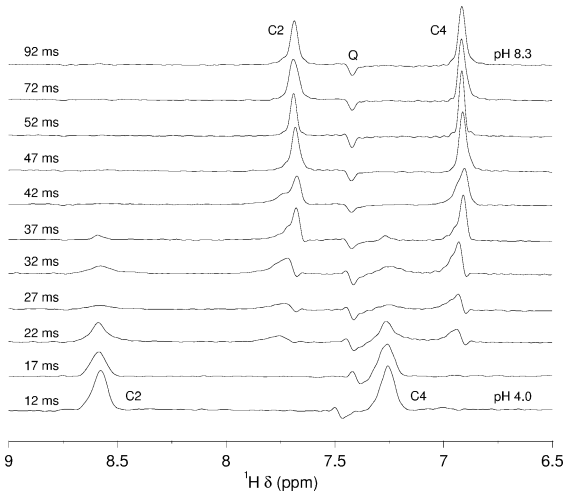

Figure 4. 500 MHz *N*-acetyl-histidine NMR spectra recorded following a pH-jump from pH 4.0 into a solution of 0.15 M *d*-TrisDCl buffer at pH 8.5. Each spectrum is the result of a single injection. Q indicates the quadrature image of the *N*-acetyl CH_3 resonance.

2. Histidine pH Jump Experiments. The imidazole ring of N−Ac−His exhibits two signals in the aromatic region of the ^{1}H NMR spectrum corresponding to the C2 and C4 protons. Their chemical shifts are sensitive to pH, moving from 8.57 to 7.71 ppm (C2) and from 7.24 to 6.92 ppm (C4) across a pH range from 4.0 to 8.3. The deprotonation of the imidazole ring is fast both on the NMR time scale (so that a single resonance at the weighted average chemical shift is anticipated for each of the ring protons) and on the time scale of the injection. This experiment provides a method of following the injection event through a chemical reaction and should give more information on the mixing efficiency than was possible by the use of video photography.

The spectra shown (Figure 4) are pseudo real-time, each involving a separate injection with a different postinjection delay, using an acquisition time of 51.2 ms. The minimum delay between the end of the injection and signal acquisition is 12 ms because of the time required for the water suppression sequence. As the delay is increased, the low pH C2 and C4 proton resonances lose intensity and disappear completely by 42 ms. The signals from the Tris-buffered high pH state (7.71 and 6.92 ppm respectively) are well resolved and have correct phases by 47 ms. Mixing thus appears to be complete at this time point after the injection event. When reactions take place in the NMR sample while a FID is being recorded, resonances arising from the initial state suffer lifetime broadening and phase shifts appear for the lines of the final state due to its formation at different times during signal acquisition.[10,21] Minor manifestations of these effects can be seen, but only in the intermediate time-period spectra (22−37 ms), supporting the conclusion that the pH jump is complete by 47 ms. Due to the solution-buffering actions of the N−Ac−His carboxyl group and the added Tris at their respective pK_a values, no intermediate pH would be realistically accessible to the N−Ac−His at any point within the tube.

This pH jump experiment was performed in the presence of Tris buffer in order to attain a complete ionization state change of the imidazole ring. An even more demanding test of the mixing efficiency was subsequently devised by performing a pH jump in the absence of buffer from the fully protonated state

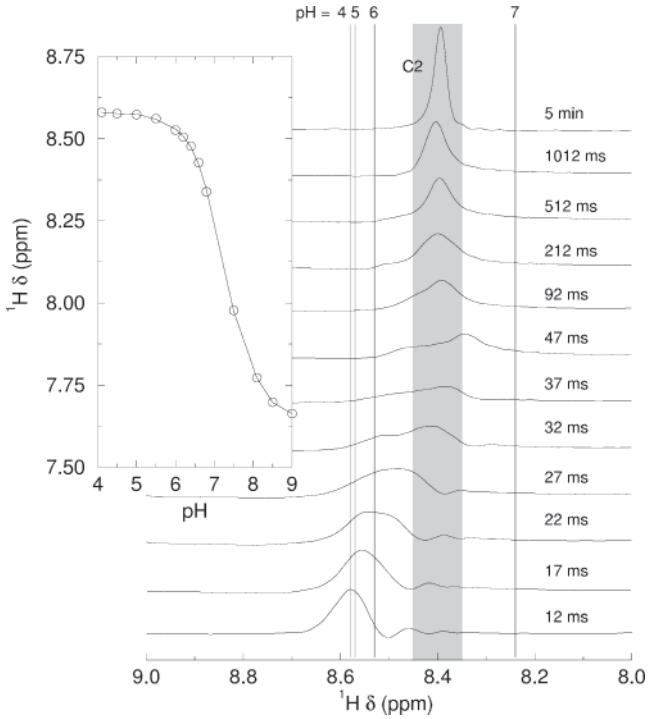

Figure 5. 500 MHz *N*-acetyl-histidine NMR spectra recorded following a pH-jump into the pK_a region, showing just the C2 proton signal. 50 μL sodium deuterioxide solution was injected into 280 μL histidine solution at pH 4.2. The four vertical lines indicate the chemical shifts of the C2 proton at the pH values shown. The shaded region shows the chemical shift region spanned by a difference in pH of ±0.2 units from the final pH. The inset shows the titration curve for the chemical shift of the C2 proton of *N*-acetyl-histidine.

(pH 4.2) to a pH (~6.5) close to the pK_a of the imidazole group, where the chemical shifts of the imidazole protons signals are highly sensitive to minor variations in pH (Figure 5). The C2 proton resonance, initially in the pH 4.2 solution (spectrum at 12 ms), was found to broaden and shift as time progressed (17−47 ms), finally emerging as a sharp peak (at 92 ms and later times).

As the imidazole deprotonation equilibrium is expected to be very fast, the observation of several peaks with similar chemical shifts in the interval 27−47 ms suggests that there are small differences in pH in different regions of the NMR tube during the mixing process. This observation can be interpreted as being the result of a highly collimated jet of injectant solution (as observed in Figure 3) causing a very rapid pH change along the central axis of the tube followed by further turbulent mixing as the injected liquid hits the base of the Shigemi tube and rebounds up the sides of the tube. Interestingly, the sensitivity of the entire procedure even permits the observation of a chemical shift overshoot (37−47 ms), which presumably results from a larger, transient change in pH arising from localized regions of the sample coming into contact with the incoming jet of high-pH sodium deuterioxide. Using the titration curve for the chemical shift of the C2 proton signal, the variation of pH within the NMR tube was found to be less than ±0.2 pH units beyond the 32 ms time point. (Figure 5, gray-shaded region). As most pH jump experiments will involve the use of buffers and, since even when unbuffered, the variation in pH across the sample is small, it is clear that our device offers remarkably efficient mixing even under demanding conditions.

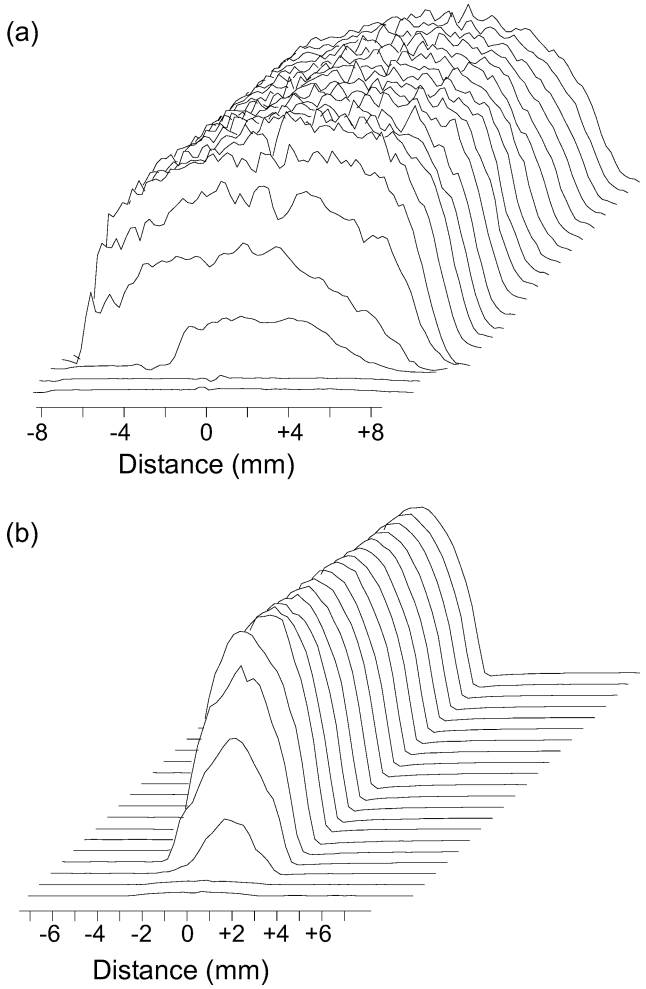

Figure 6. 500 MHz 1D NMR images following an injection of 50 μL H_2O into 280 μL D_2O, showing the distribution of protons after the injection event. Part (a) shows a series of real-time NMR images taken along the *z*-axis (the right-hand side of the spectrum corresponds to the top of the NMR sample), whereas (b) shows images along the *x*-axis. The spectra were recorded at 10 ms intervals. The horizontal axes in both figures have been calibrated as a distance from the center of the RF coil.

3. One-Dimensional ^{1}H NMR Imaging. Using NMR imaging techniques, it is possible to study the distribution of molecular species during an injection event so as to provide spatial, as well as temporal, information. A series of real-time 1D images of the NMR tube following an injection of H_2O into D_2O was recorded at 10 ms intervals. These images were taken along the *x*- and *z*-axes of the NMR tube, allowing determination of the extent of radial and axial mixing, respectively. No signal is observed at 0 and 10 ms in either set of images (Figure 6). At 20 ms, a small signal appears, which gradually increases until 50 ms, and then remains constant. Gentle layering of H_2O on top of D_2O in an NMR tube was used to establish that the right-hand side of the image corresponded to the top of the NMR tube sample region. The *z*-axis images (Figure 6a) thus, remarkably, show the progress of the injected H_2O flowing down the NMR tube beginning at 20 ms and continuing in subsequent images. This finding is confirmed by the width of the *x*-axis images (Figure 6b), in which the radial distribution of the injected H_2O is concentrated close to the *z*-axis ($x = 0$) at 20 ms, becoming broader up to a time of about 50 ms as the mixing proceeds. The full width at half-maximum height of the *x*-axis images increases from 1.75 mm to 3.5 mm over the 40 ms time period following the injection. Taken together, the two sets of images support the idea of a jet of liquid passing down the center of the tube and flowing back up the sides so effecting efficient mixing. It can be concluded that mixing is complete between 40 and 50 ms, in good agreement with the previous series of experiments. The experiment was repeated (results not shown) using 1.5 M calcium chloride in water in place of pure H_2O to determine the mixing time for a solution with viscosity similar to that of the 8 M guanidine HCl solution used in the real-time refolding experiment on hen lysozyme described below. In agreement with the fluorescence measurements above, mixing was found to be complete within 100 ms.

Repeating the experiments in which pure H_2O is injected into D_2O using a standard round-bottomed NMR tube shows that mixing does not go to completion, even after several seconds, as there is an excess of injected solution at the top of the tube and unmixed solution at the bottom of the tube (data not shown). This observation supports the argument that the flat bottom of the susceptibility-matched Shigemi tube significantly improves the mixing process.

B. Applications to Folding. The kinetic aspects of protein folding have been widely studied using a variety of stopped-flow and real-time methods.[5,35] Optical detection techniques such as circular dichroism and fluorescence spectroscopy have been widely employed to probe secondary structure formation or changes in the environment of side chain chromophores.[36] Using quenched-flow H/D pulse-labeling techniques, NMR has played an important role in probing the kinetic events involved in the formation of compact conformations of the polypeptide backbone.[6,37] An additional complementary application of NMR has been to monitor, directly in real time, the resonances of side chain nuclei as folding proceeds.[4,7,8] Such experiments have provided residue-specific insights into the structural transitions occurring during protein folding, especially when transient intermediates are present. In such cases, faster and more efficient mixing is usually desirable to improve signal-to-noise ratios or to probe intermediates that may exist at even earlier times.[4,5,26,27] Two time-resolved protein folding experiments that benefit from using the new injection device are described here.

1. Real-Time Refolding of Hen Egg White Lysozyme. The injection system allows one to rapidly trigger the refolding of non-native states of proteins, a process that can be followed in real-time by monitoring individual site-specific proton resonances in a series of transient spectra. With the inclusion of the optical fiber, it is possible to exploit CIDNP effects, where polarization is generated in solvent-exposed side chains of the aromatic amino acid residues tyrosine, tryptophan and histidine by a photochemical reaction with a suitable dye such as FMN. The reactions proceed via radical pair intermediates, which leave in their wake a spin polarization of the protons in the reactive side chains, detectable as changes in the amplitude of the NMR signals.[12] Polarized signals from nonexchangeable protons in tyrosine and tryptophan residues have previously been reported in refolding experiments on lysozyme,[13] but we believe this is

(35) Roder, H.; Elöve, G. A.; Shastry M. C. R. In *Mechanisms of Protein Folding*, Pain, R. H., ed.; Oxford University Press: New York, **2000**, 65−95.
(36) Dobson, C. M.; Evans, P. A.; Radford, S. E. *Trends Biochem. Sci.* **1994**, *19*, 31−37.
(37) Redfield, C.; Poulsen, F. M.; Dobson, C. M. *Eur. J. Biochem.* **1982**, *128*, 527−531.

the first time that signals from the exchangeable (indole) protons have been reported under real-time conditions.

Figure 7a shows the evolution of peaks in the indole region of the ^{1}H CIDNP spectrum after injection of GdnHCl-denatured HEWL into a refolding buffer. The initial (8.0 M) and final (1.5 M) GdnHCl concentrations were chosen to decelerate the refolding in order to observe the process in greater detail. Over the course of the measurement, there is a significant change in the appearance of the spectrum; the broad signal resulting from the tryptophan indole protons of the unfolded state (10.1 ppm) in the first few spectra is rapidly replaced by two sharp resonances at chemical shifts (10.20 and 10.75 ppm) appropriate for two tryptophan indole protons in the native state. These two signals, known from their assignment[37] to be from the two most solvent-accessible of the six tryptophan residues in the protein,[38] Trp 62 and Trp 123, are accompanied by a variety of resonances in the aromatic region of the spectrum (not shown) arising from tryptophan and tyrosine ring protons.[38] The greater amplitude of the resonance from Trp 62 compared to Trp 123 reflects its greater accessibility and therefore reactivity toward FMN. Note that by the time the first spectrum was recorded (113 ms delay), the mixing of solutions and dilution of the denaturant had gone to completion, as determined by the fluorescence and imaging tests described above.

Optical stopped-flow measurements on HEWL indicate a biphasic recovery of the native state, with a minor component (~5%) folding via a "fast track";[39−41] the two pathways are, however, difficult to distinguish when refolding is carried out at a final GdnHCl concentration of 1.5 M because of their similar kinetics.[40] Moreover, at this final denaturant concentration, the stopped-flow intrinsic fluorescence shows little overshoot, again suggesting that biphasic kinetics due to a significant fast track is minimized. The peak heights of the indole protons of Trp 62 and Trp 123 were therefore fitted to a biexponential function, with *one* component corresponding to the growth of the native state signals and the other to the decay of the polarization due to photodepletion of dye in the NMR coil region (Figure 7(b)). The refolding time constants obtained from these data were essentially equal: 2.38 ± 0.1 s for Trp 62 and 2.24 ± 0.1 s for Trp 123. This value compares with a time constant of 1.1 s measured using fluorescence;[40] the slower overall rate of folding can be attributed to the use of a higher (8.0 as opposed to 6.0 M) initial GdnHCl concentration. Previous CIDNP experiments, in which the nonexchangeable aromatic proton signals were studied in D_2O solution, were unable to discriminate the resonances of the two tryptophan residues because of severe overlap in the aromatic region of the CIDNP spectra.[16]

In contrast, the unfolded HEWL tryptophan indole signal at 10.1 ppm decays with somewhat faster kinetics, with a time constant of 0.57 ± 0.1 s. The more rapid disappearance of this peak may be related to the fact that in the unfolded state up to six tryptophan residues contribute to the signal,[42] three of which (Trp 28, Trp 108, and Trp 111) are part of the hydrophobic core in the native state. The rapid disappearance of the unfolded Trp indole CIDNP signal suggests an early hydrophobic collapse

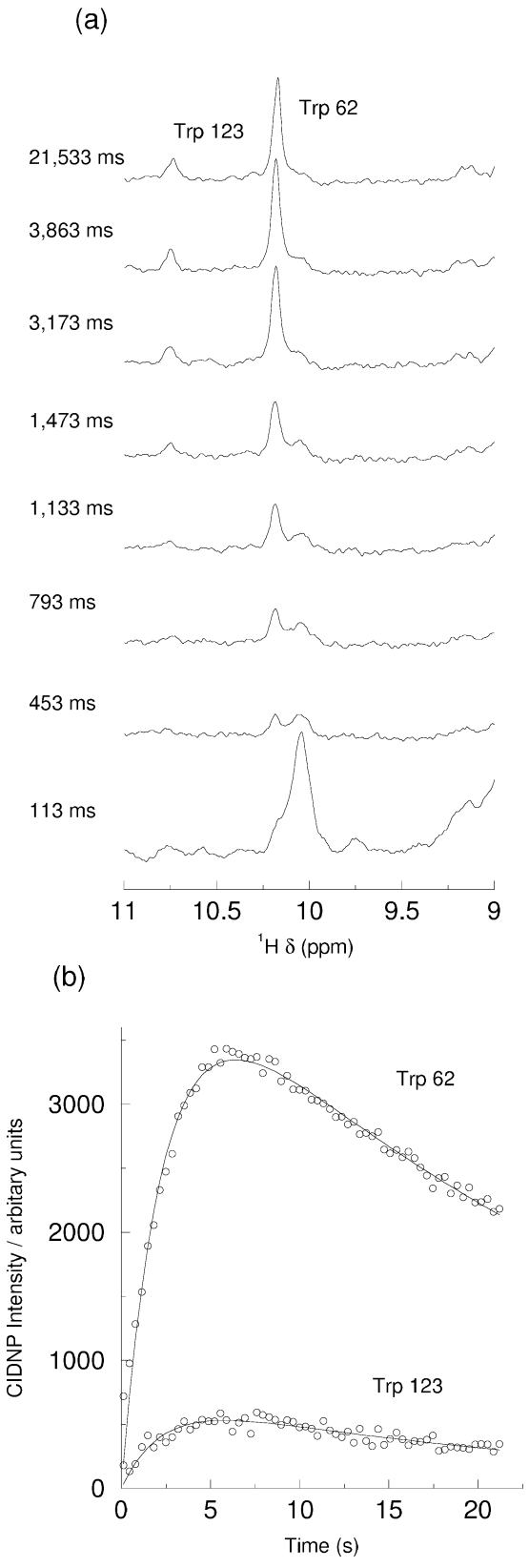

Figure 7. 600 MHz real-time refolding of HEWL following a 6.6-fold dilution from 8.0 M guanidine HCl. The complete real-time series (a) is the result of averaging over four injections, with laser illumination applied for 100 ms before each scan. The labels indicate the delays between the end of the injection and the start of signal acquisition. Part (b) shows the tryptophan indole proton peak heights as a function of time following the injection event. The solid lines are the result of fitting the data to a double exponential curve.

(38) Hore, P. J.; Kaptein, R. *Biochemistry* **1983**, *22*, 1906−1911.
(39) Radford, S. E.; Dobson, C. M.; Evans, P. A. *Nature* **1992**, *358*, 302−307.
(40) Kiefhaber, T. *Proc. Natl. Acad. Sci. U.S.A.* **1995**, *92*, 9029−9033.
(41) Matagne, A.; Dobson, C. M. *Cell. Mol. Life. Sci.* **1998**, *54*, 363−371.
(42) Lyon, C. E.; Jones, J. A.; Redfield, C.; Dobson, C. M.; Hore P. J. *J. Am. Chem. Soc.* **1999**, *121*, 6505−6506.

during the process of refolding, evidence for which has been reported in numerous studies.[13,41,43] Although preliminary, our observation that the indole peak of Trp 62 fails to show an appreciable lag in reaching the native state when compared with Trp 123 suggests that Trp 62 could have significant solvent-accessiblity in the non-native hydrophobic clustering in the denatured state.[44] Further work in determining the accessibility of Trp 62 in hydrophobic clusters using equilibrium and real-time indole-proton CIDNP is currently in progress, but the present observation provides the crucial evidence that it is possible to observe the resonances of exchangeable protons under refolding conditions.

As mentioned above, a very slow decay is observed for the CIDNP intensities of both tryptophan residues, with similar time constants: 27.5 ± 1.0 s for Trp 62 and 23.2 ± 1.0 s for Trp 123 (Figure 7b). This decay is due to local photobleaching of the photosensitizer dye FMN,[45] as a large number of laser pulses were applied within a relatively short period of time (64 laser flashes within 23 s). Control experiments on native HEWL with much longer intervals between laser flashes showed very little loss of signal intensity (data not shown). The decreased flash rate allows time for fresh flavin and dissolved oxygen to diffuse into the coil region, respectively to replace and to re-oxidize photoreduced flavin molecules. This implies that the slow signal decay observed in the real-time experiments is indeed a function of photobleaching rather than, for example, photochemical damage to the protein. Hence, the photoreduction does not interfere with the much faster folding reaction and can easily be distinguished from it.

2. CIDNP Pulse Labeling Study of a Partially Folded Species of Hen Egg White Lysozyme. The CIDNP pulse labeling technique can provide information on unfolded or partially folded states of proteins through the transfer of nuclear polarization from the unfolded state to the native state by rapid refolding.[14,46] This method exploits the high-resolution spectrum of the native state to obtain information on the denatured state whose spectra are often poorly resolved by comparison.[5,18] It is a demanding experiment, requiring the folding to be faster than the spin−lattice relaxation of the residues involved in order that the nuclear polarization can be detected with adequate sensitivity. CIDNP pulse labeling results for lysozyme, partially denatured using 1,1,1-trifluoroethanol (TFE) are shown in Figure 8. In the presence of 45% TFE (v/v), HEWL forms a partially structured state with a high degree of helical structure.[47] In the pulse labeling procedure described previously,[14] nuclear polarization is induced in a solution of the unfolded state by means of a photochemical reaction between FMN and solvent-accessible tyrosine, tryptophan and histidine residues. The protein is then rapidly folded back to the native state by injection into a refolding medium and the nuclear polarization detected. The technique is of particular use when the spectrum of the denatured state has such poor resolution that individual resonances cannot be distinguished.[14]

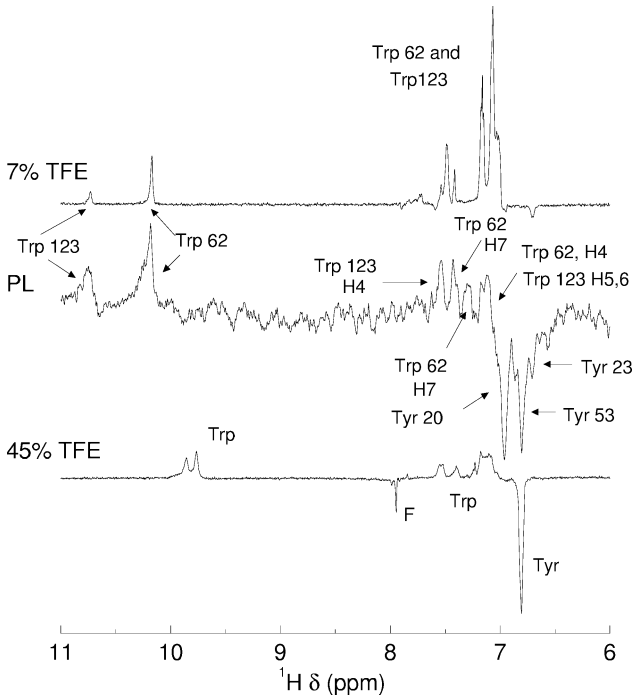

Figure 8. CIDNP pulse-labeled spectrum of HEWL diluted from 45% (v/v) to 7% TFE. The spectrum was recorded at 600 MHz, averaged over four light and dark pairs. Laser illumination for 500 ms was used, with an injection time of 50 ms and postinjection delay of 100 ms. Top: equilibrium CIDNP spectrum of lysozyme in 7% TFE. Bottom: equilibrium CIDNP spectrum of lysozyme in 45% TFE. Centre: pulse-labeled CIDNP spectrum. The peaks corresponding to the solvent accessible tyrosine and tryptophan residues are shown. F denotes a signal arising from polarized flavin.

Figure 8 shows the results of the pulse labeling experiment on HEWL (middle) together with spectra of HEWL denatured in 45% TFE (bottom) and refolded in 7% TFE (top) following a 6.6-fold dilution. The presence of a low concentration of TFE in the final solution increases the rate of refolding significantly,[48] and reduces relaxation losses.[14] The pulse-labeled spectrum contains resonances with chemical shifts corresponding to those of the refolded state (in 7% TFE) but with NMR intensities corresponding to the denatured state (in 45% TFE). What is immediately striking is the similarity of the 7% TFE and pulse-labeled spectra in the region above 7 ppm that contains the tryptophan resonances and the dissimilarity of the two spectra below 7 ppm where the tyrosine resonances appear. Three emissive signals are clearly visible around 7 ppm in the pulse-labeled spectrum, corresponding to all three of the tyrosine residues in the protein which are evidently exposed in the TFE state, but (almost completely) buried in the native state of HEWL (only Tyr 23 shows a small emissive polarization in the 7% TFE spectrum). It is important to note that it is not possible to tell from the poorly resolved spectrum in 45% TFE how many of the tyrosine residues are exposed in this state. Resonances from two tryptophan indole protons (Trp 62 and 123) are visible above 10 ppm, indicating that these, and only these, tryptophans are solvent-exposed in the 45% TFE state, as is the case in the native state. The tryptophan residues that normally constitute the native hydrophobic core (Trp 28, Trp

(43) Morgan, C. J.; Miranker, A.; Dobson, C. M. *Biochemistry* **1998**, *37*, 8473−8480.
(44) Klein-Seetharaman, J.; Oikawa, M.; Grimshaw, S. B.; Wirmer, J.; Duchardt, E.; Ueda, T.; Imoto, T.; Smith, L. J.; Dobson, C. M.; Schwalbe, H. *Science* **2002**, *295*, 1719−1722.
(45) Maeda, K.; Lyon, C. E.; Lopez, J. J.; Cemazar, M.; Dobson, C. M.; Hore, P. J. *J. Biomol. NMR* **2000**, *16*, 235−244.
(46) Lyon, C. E. *D. Philos. Thesis*, University of Oxford, Oxford, United Kingdom, **1999**.
(47) Buck, M.; Radford, S. E.; Dobson, C. M. *Biochemistry* **1993**, *32*, 669−678.
(48) Lu, H.; Buck, M.; Radford, S. E.; Dobson, C. M. *J. Mol. Biol.* **1997**, *265*, 112−117.

108, Trp 111) are thus found to be solvent-inaccessible in the TFE-denatured state as well. This result suggests that significant nativelike character may persist in the TFE state despite its different secondary structure content. The observation of native-like properties in such denatured states has been postulated previously[49] and the present experiment suggests that NMR experiments might be able to provide detailed information about such structures, even in cases where the NMR spectra are very poorly resolved.

The results described in this paper demonstrate an injection technique capable of efficient and rapid mixing of solutions such that sharp, correctly phased NMR signals can be obtained 50 ms after the injection. The power and sensitivity of NMR as reflected in the chemical shift changes and ^{1}H images permit even minor deficiencies in the homogeneity of the mixing to be detected. The equipment is constructed from simple components, requires no spectrometer modifications, in conjunction with CHESS solvent suppression yields high quality ^{1}H spectra of solutes in H_2O solution, and allows real-time experiments on proteins to be performed. Other applications to a wide variety of chemical and photochemical processes can be envisaged.

Acknowledgment. We would like to thank the EPSRC, BBSRC, and MRC for financial support through the Oxford Centre for Molecular Sciences (OCMS). We thank Dr. A. Blamire, Dr. K. Maeda, Dr. C. E. Lyon, Dr. J. J. Lopez, and Dr. A. Matsuyama for helpful discussions and assistance. We would also like to thank Mr. L. Kuhn for preliminary experiments, Mr. I. Kuprov for the table of contents graphic and Mr. M. Myles for the construction of the injection insert. Further funding was provided by the EU (RTD Project No. HPRI-1999-CT-50006), by INTAS (Project No. 01-2126) and by the Royal Society. K. H. M. was supported by a Chevening Scholarship (British Foreign and Commonwealth Office) and the OCMS. The research of C. M. D. is supported in part by a Program Grant from the Wellcome Trust.

JA036357V

(49) Chiti, F.; Taddei, N.; Webster, P.; Hamada, D.; Fiaschi, T.; Ramponi, G.; Dobson C. M. *Nat. Struct. Biol.* **1999**, *6*, 380−387.